Potent synergy of dual antitumor peptides for growth suppression of human glioblastoma cell lines

Eisaku Kondo,[1] Takehiro Tanaka,[1] Takayoshi Miyake,[1] Tomotsugu Ichikawa,[2] Masahiko Hirai,[4] Masaki Adachi,[4] Kazuhiro Yoshikawa,[5] Koichi Ichimura,[1] Nobuya Ohara,[1] Akiyoshi Moriwaki,[3] Isao Date,[2] Ryuzo Ueda,[6] and Tadashi Yoshino[1]

Departments of [1]Pathology and [2]Neurological Surgery, Okayama University Graduate School of Medicine, Dentistry and Pharmaceutical Sciences; [3]Department of Human Nutrition, Chugokugakuen University, Okayama, Japan; [4]R&D Center, Katayama Chemical Industries Co., Ltd., Osaka, Japan; [5]Research Complex for the Medicine Frontiers, Aichi Medical University School of Medicine, Aichi, Japan; and [6]Department of Medical Oncology and Immunology, Nagoya City University Graduate School of Medical Sciences, Nagoya, Japan

Abstract

Molecular targeting agents have become formidable anticancer weapons, which show much promise against the refractory tumors. Functional peptides are among the more desirable of these nanobio-tools. Intracellular delivery of multiple functional peptides forms a basis for potent, non-invasive mode of delivery, providing distinctive therapeutic advantages. Here, we examine growth suppression efficiency of human glioblastomas by dual-peptide targeting. We did simultaneous introduction of two tumor suppressor peptides ($p14^{ARF}$ and $p16^{INK4a}$ or $p16^{INK4a}$ and $p21^{CIP1}$ functional peptides) compared with single-peptide introduction using Wr-T-mediated peptide delivery. Wr-T-mediated transport of both $p14^{ARF}$ and $p16^{INK4a}$ functional peptides (p14-1C and p16-MIS, respectively) into human glioblastoma cell line, U87ΔEGFR, reversed specific loss of *p14* and *p16* function, thereby drastically inhibiting tumor growth by >95% within the first 72 h, whereas the growth inhibition was ~40% by p14 or p16 single-peptide introduction. Additionally, the combination of p16 and $p21^{CIP1}$ (p21-S154A) peptides dramatically suppressed the growth of glioblastoma line Gli36ΔEGFR, which carries a missense mutation in *p53*, by >97% after 120 h. Significantly, our murine brain tumor model for dual-peptide delivery showed a substantial average survival enhancement ($P < 0.0001$) for peptide-treated mice. Wr-T-mediated dual molecular targeting using antitumor peptides is highly effective against growth of aggressive glioblastoma cells in comparison with single molecule targeting. Thus, jointly restoring multiple tumor suppressor functions by Wr-T-peptide delivery represents a powerful approach, with mechanistic implications for development of efficacious molecular targeting therapeutics against intractable human malignancies. [Mol Cancer Ther 2008;7(6):1461–71]

Introduction

Steady advancements in cancer chemotherapies have ameliorated prognoses for late-stage disease; however, there remain numerous malignancies that are refractory to known therapies. Consequently, cutting-edge molecular strategies such as small interfering RNA, humanized antibodies, and small-molecule inhibitors have gained great notice for their breakthrough potential (1–5). However, the intractable malignancies bear multiple genetic alterations; thus, treatment comprising a plurality of targeting agents is critically necessary. A prominent example is human glioblastoma, which is highly recalcitrant to conventional chemotherapy. Importantly, glioblastoma is often noted for its expressional losses in such tumor suppressors as the INK4 family of genes (p14, p15, p16, p18, and p19; refs. 6–9). Especially, *p16* and *p14* stand out due to their pronounced rates of deletion, point mutation, and aberrant methylation; both genes are encoded at the same CDKN2A locus (10). In spite of amino acid sequence differences, comapping $p16^{INK4a}$ and the $p14^{ARF}$, either through the regulatory role of CDK4/CDK6 or p53, share important cell cycle control and apoptotic functions leading to tumor suppression. Accordingly, we hypothesize that joint functional restoral of p16- and p14-based or p21-based tumor suppression by dual-peptide transport may dramatically enhance the antitumor effect, in preference to the single-peptide regime, on aggressive malignant tumors. Here, we report the successful implementation of such a system, consisting of our highly efficacious peptide/protein transporter (Wr-T; ref. 11) and potent p16 and p14 or p21 antitumor peptides, using human glioblastoma cells as an *in vitro* and *in vivo* model in pursuit of an advanced anticancer therapy.

Materials and Methods

Peptide Synthesis

All peptides, including Wr-T, peptide A, peptide B, peptide C, and pep-1 (12) listed in Fig. 1, p14-1C and

Received 8/29/07; revised 2/21/08; accepted 4/2/08.

Grant support: Kiban (C) Grants-in-Aid for Scientific Research, Japanese Ministry of Education, Culture, Sports, Science and Technology grant 16590279.

The costs of publication of this article were defrayed in part by the payment of page charges. This article must therefore be hereby marked *advertisement* in accordance with 18 U.S.C. Section 1734 solely to indicate this fact.

Note: E. Kondo and T. Tanaka contributed equally to this work.

Requests for reprints: Eisaku Kondo, Department of Pathology, Okayama University Graduate School of Medicine, Dentistry and Pharmaceutical Sciences, 2-5-1 Shikata-cho, Okayama 700-8558, Japan.
Phone: 81-86-235-7152; Fax: 81-86-235-7156.
E-mail: ekondo@md.okayama-u.ac.jp

doi:10.1158/1535-7163.MCT-07-2010

transporter	protein docking domain	spacer	PTD
Wr-T	KETWWETWWTEWWTEWSQ	GPG	rrrrrrrrr (*r=D-Arg)
peptide A	KETWWETWWTEWSQ	GPG	rrrrrrrrr
peptide B	KETWWETWWTEWWTEWSQ		rrrrrrrrr
peptide C	KET WWETWWTEWWTEWSQ	GPG	PKKKRKV
Pep-1	KET WWETWWTEWSQ		PKKKRKV

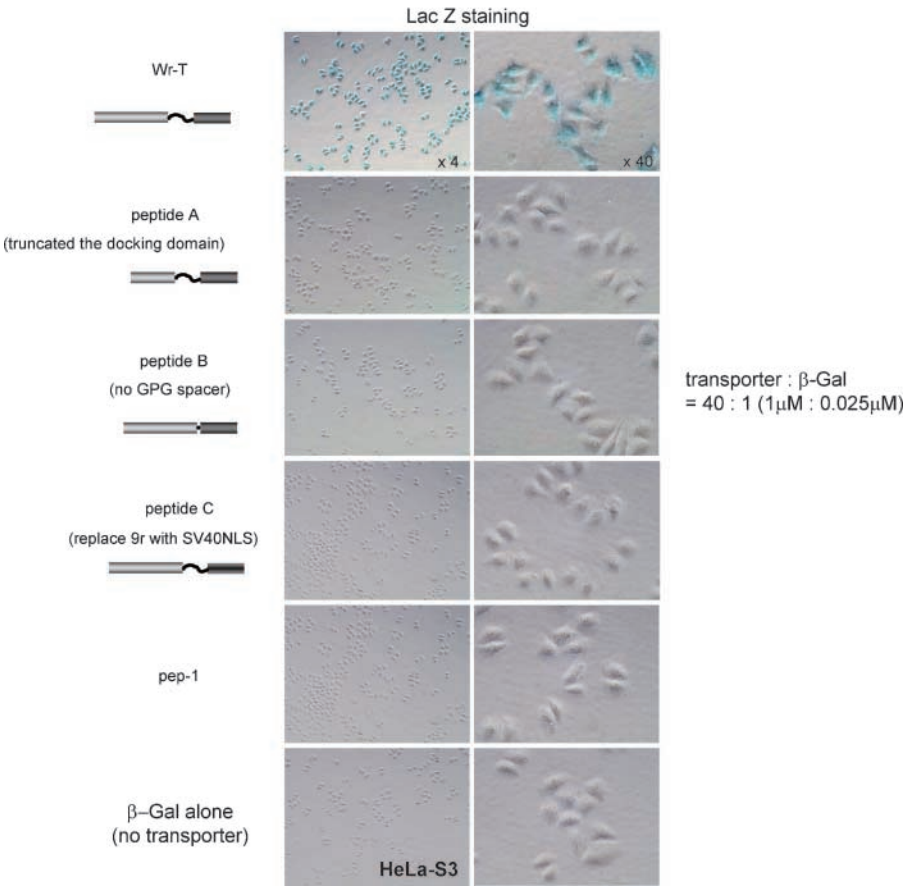

Figure 1. Functional properties of Wr-T peptide/protein transporter. The indicated peptides (Wr-T, peptide A, peptide B, peptide C, and pep-1) were synthesized to functionally characterize each domain of the Wr-T transporter based on efficiency of incorporation of the β-Gal tetramer in HeLa-S3 cells. *r*, D-arginine. Incorporated signal of β-Gal was developed in HeLa cells by LacZ staining. Then, 1 μmol/L of each synthesized peptide was mixed with 25 nmol/L β-Gal tetramer, and intracellular uptake of β-Gal was evaluated by LacZ staining 3 h after treatment with each mixture.

p16-MIS in Fig. 2, and p21-S154A in Fig. 4, were synthesized at Sigma Genosys by standard Fmoc chemistry on an ABI 433A Peptide Synthesizer (Applied Biosystems). Crude peptides were purified by reverse-phase high-performance liquid chromatography over a C18 preparatory column (Varian). Peptide identities were confirmed by mass spectrometry. All peptides precipitated from trifluoroacetic acid solutions are trifluoroacetic acid salts. We prepared the HCl form of peptides following high-performance liquid chromatography purification for both *in vitro* and *in vivo* applications. For synthesis of p16-MIS, p14-1C, and p21-S154A, the oligo amino acid residues (reported in refs. 13–16) were defined as the functional core of the peptide, although cores themselves tended to be insoluble (e.g., the core p16 sequence, ''MIS,'' FLDTLVVLHR has a hydrophobicity of 69.2%). Consequently, fusion with a run of nine D-arginines (r9) was used for reduction of hydrophobicity (e.g., to 40%) and for constituting a protein transduction domain (PTD; ref. 11).

Peptide Transduction

To introduce the peptide mixture for *in vitro* and *in vivo* growth suppression, the Wr-T transporter and each functional peptide including p16-MIS, p14-1C, and p21-S154A were mixed as described previously (11). For the first assay to examine functional properties of the transporter-encoded peptide sequences, 1 μmol/L of each peptide (shown in Fig. 1) was mixed with 25 nmol/L β-galactosidase (β-Gal) tetramer (total molecular weight was ~485 kDa; Sigma-Aldrich), and the complex was added to the medium of HeLa-S3 cells cultured in a 24-well polystylane culture plate and incubated for 24 h at 37°C in CO_2 incubator, and LacZ staining was done to examine the incorporation of the β-Gal

by each transporter peptide. In other *in vitro* assays, 3.5 μmol/L Wr-T (final concentration) was used to form each complex with 3 μmol/L cargo peptide. A peptide complex was left for 30 min at room temperature, which was then directly added to cell culture medium. For *in vitro* growth assay of each glioblastoma cell line, 2×10^4 cells were prepared for peptide transduction as a starting point. For *in vivo* peptide delivery to mouse brain tumor, the dual-peptide complexes (20 nmol Wr-T mixed with 20 nmol p16-MIS to form Wr-T/p16 complex and 20 nmol Wr-T mixed 20 nmol p14-1C for Wr-T/p14 complex) were suspended in PBS (total volume: 100 μL) and were injected into the right ventricle of the murine heart. As a control, in parallel, 100 μL PBS without peptide was injected into mice.

Cells

Human glioblastoma cell lines U87ΔEGFR, Gli36ΔEGFR, and SF767 were mainly used for the present study. U87ΔEGFR carries a mutant epidermal growth factor receptor deleted for 267 amino acids in the extracellular domain; this line was suspended in DMEM with 10% FCS containing 0.5 mg/mL G418 (17). Gli36ΔEGFR was established by retroviral transfer of mutant EGFR as described previously and was suspended in DMEM supplemented with 10% FCS containing 0.5 g/mL puromycin (18). SF767 was suspended in DMEM with 10% FCS (19). U87MG, U251, AO2, SK-MG-1, T98 (nongenetically engineered human glioma cell lines kindly provided by Dr. A. Natsume, Department of Neurosurgery, Nagoya University Graduate School of Medicine), HeLa (cervical carcinoma), Hs578 (breast carcinoma purchased from the American Type Culture Collection), peripheral blood mononuclear cells from healthy donors (lymphocytes), normal human dermal fibroblasts, and normal hepatocytes isolated from murine liver were also used for peptide

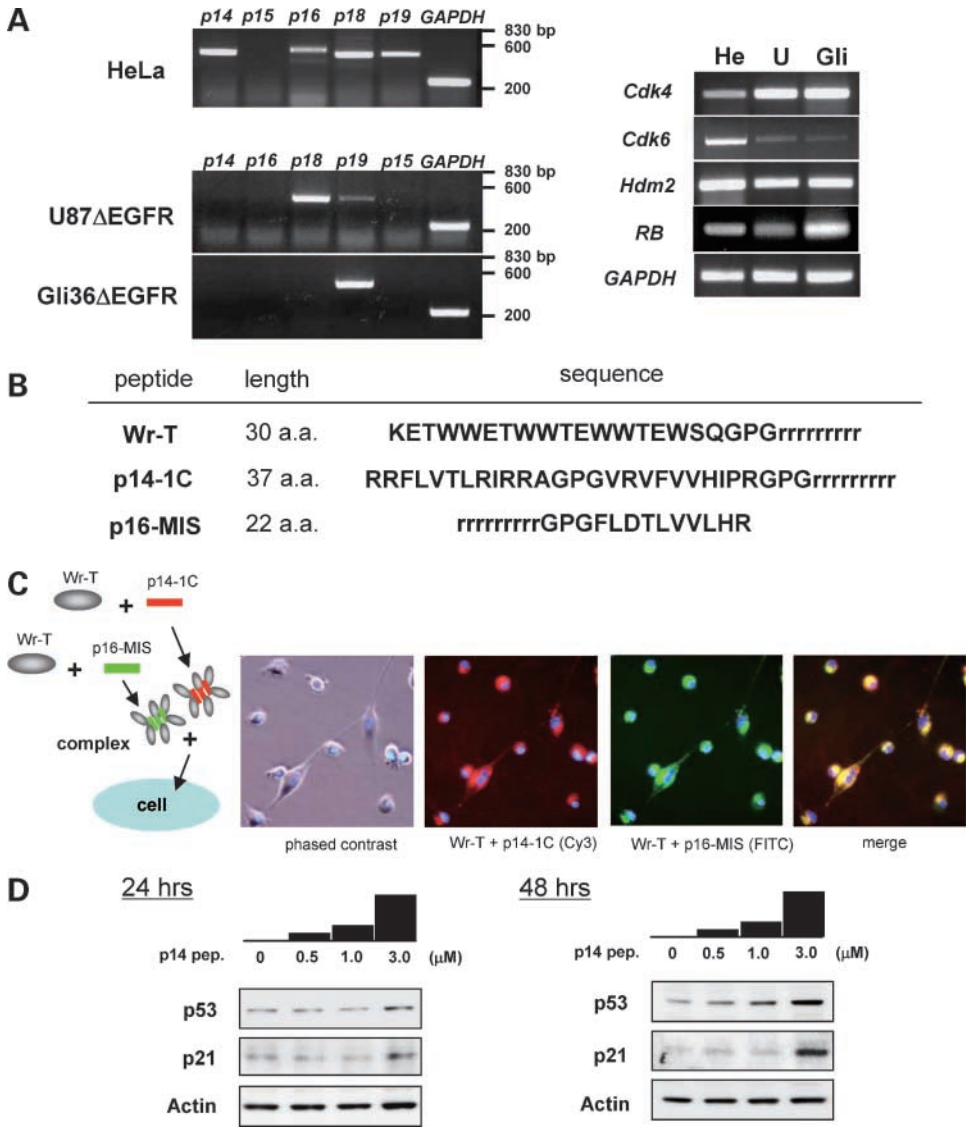

Figure 2. Loss of $p14^{ARF}$ and $p16^{INK4a}$ expression in two human glioblastoma cell lines and Wr-T-mediated intracellular uptake of p14 and p16 functional peptides. **A,** endogenous mRNA expression of *INK4* tumor suppressor gene family by reverse transcription-PCR in two human glioblastoma cell lines, U87ΔEGFR and Gli36ΔEGFR. Expression was also examined for cell cycle pathway genes converging to *RB, Cdk4, Cdk6*, and *Hdm2*. **B,** sequence design of the p14 functional peptide ''p14-1C'' and p16 functional peptide ''p16-MIS.'' **C,** U87ΔEGFR cellular uptake of Cy3-labeled p14-1C and FITC-labeled p16-MIS mixed with Wr-T shown by fluorescence microscope. p14-1C (3 μmol/L) and p16-MIS (3 μmol/L) were each mixed with Wr-T (3.5 μmol/L). **D,** p14-1C delivered by Wr-T (7 μmol/L) restored p53 protein in U87ΔEGFR cells in a dose- and time-dependent manner. Immunoblot revealed increasing amounts of p53 and p21 proteins paralleling the p14-1C concentration. *Right,* 24 h post-introduction; *left,* 48 h post-introduction.

delivery assays to examine either the growth-inhibitory effect or cytotoxic effect (shown as Supplementary Data).[7]

Reverse Transcription-PCR

Total RNA (5 μg) was extracted from each human glioma cell line or from HeLa, Hs578, and murine hepatocyte cells with a commercial kit (RNA Quick; Qiagen). cDNA was synthesized from the RNA product using an oligo(dT) primer and cDNA synthesis kit (SuperScript first-strand synthesis system; Invitrogen). Reverse transcription-PCR was done with Z-Taq polymerase (Takara Bio): amplification conditions were 98°C for 3 min followed by 26 cycles of 98°C for 2-s denaturation, 68°C for 15-s extension, and final extension at 72°C for 10 min. The sense/antisense primer sequences for human $p14^{ARF}$ were 5′-ATGGTGCGCAGGTTCTTGG-3′ and 5′-TGCGGGCATGGTTACTGCCTC-3′, respectively, and those for *Hdm2* were 5′-ATGTGCAATACCAACATGTC-3′ and 5′-CTAGGGGAAATAAGTTAG-3′, respectively. The antisense primer for murine $p19^{ARF}$ was 5′- CTATGCCCGTCGGTCTGGGC-3′; the sense primer was the same as that of the human $p14^{ARF}$. The sense/antisense primers for the murine p16 were 5′-ATGGAGTCCGCTGCAGACAG-3′ and 5′-TGCTTGAGCTGAAGCTATGC-3′, respectively. The sense/antisense primer sequences for *p16, p15, p18, p19, Cdk4, Cdk6, RB*, and *GAPDH* were reported previously (11, 20).

Immunoblotting

U87ΔEGFR cells were treated with p14-1C peptide and were lysed with SDS sample buffer. Extracts were then separated by denaturing electrophoresis on 4% to 12% bis-Tris gradient gels (Novex). Proteins were transferred to nitrocellulose and developed with the relevant primary antibodies and horseradish peroxidase–conjugated goat anti-mouse IgG (ZyMax; Zymed). Primary antibodies were mouse anti-p53 monoclonal antibody (DO7; DAKOCytomation), mouse anti-p21 monoclonal antibody (Santa Cruz Biotechnology), and mouse anti-actin monoclonal antibody (Chemicon). For the dual-peptide-treated HeLa, Hs578, normal murine hepatocytes, and normal human fibroblasts, mouse anti–poly(ADP-ribose) polymerase monoclonal antibody (BD Bioscience) was used to determine apoptosis levels (shown as Supplementary Data).[7]

Fluorescence Imaging

Uptake and intracellular localization of Cy3-labeled p14-1C, FITC-labeled p16-MIS, or Atto655-labeled p21-S154A peptide were visualized in live cells by inverted fluorescence microscope (Olympus IX71-ARCEVA). Fluorescent images derived from *in vitro* assays were from cells peptide treated for 24 h. For fluorescence images of incorporated peptides, mouse brain was surgically excised after 24-h treatment with i.v. injected peptides. Brain slices (3 mm thickness) were sequentially examined by zoom stereo fluorescence microscope (Olympus SZX12) without fixation.

Transfection of p53 Genes to Glioma Cell Line

R248L mutation was generated by site-directed mutagenesis using human wild-type p53 (WT-p53) as a template. Both WT-p53 and R248L mutant p53 fragment were subcloned into pEGFP-C3 vector (Clontech Laboratories). Triplicated samples of each 1×10^5 of Gli36ΔEGFR cells were transfected either with 1 μg pEGFP-WT-p53 or pEGFP-R248L-p53 by mixing with LipofectAMINE-LTR (Invitrogen Japan) and incubated for 12 h before 0 (no UV), 10, and 15 J/m^2 UV irradiation to trigger apoptosis in response to genomic DNA damage for the assessment of *p53* function (UV wavelength, 302 nm). The percentage of apoptotic cells in each sample was calculated by triplicate counting of active caspase-3-positive apoptotic cells among 300 nuclear EGFP p53-positive cells under fluorescent microscope.

Flow Cytometry

Apoptosis assays were done with the Cy3-Annexin V staining kit (MBL) on peptide-treated U87ΔEGFR cells. Cultures were harvested by trypsinization and PBS wash, according to the manufacturer's instruction, followed by analysis using the FACScan cytometer (Becton Dickinson) and FlowJo software (Tree Star). A total of 10,000 cells comprised each sample. Cell cycle analysis was also done by FACScan using propidium iodide staining as described previously (11).

Cell Proliferation Assay

Cell growth was evaluated with the reagent 3-(4,5-dimethylthiazol-2-yl)-2,5-diphenyltetrazolium bromide (MTT; Sigma-Aldrich). Log-phase cells were seeded in 12-well collagen type I–coated plates (1×10^4 per well), allowed to adhere 24 h, and then treated with functional peptide. Following peptide introduction, cells were incubated for varying periods (24, 48, 72, 96, and 120 h) and exposed to 0.5 mg/mL MTT over a span of 4 h to permit MTT reduction. Formazan crystals were solubilized by adding a 0.01 mol/L HCl-10% SDS mixture, and absorbance was measured at 570/630 nm dual wavelength. In the growth inhibition assay of the peptide-treated Gli36-ΔEGFR, data were presented as the relative percentage cell proliferation in each sample, comparing its absorbance value with that of the nontreated control sample; data are MTT background subtracted.

Immunofluorescence

For apoptosis assay of Gli36ΔEGFR carrying WT-*p53* or mutative *p53*, the cells were stained with rabbit anti-active caspase-3 polyclonal antibody (BD Biosciences Japan) after formalin fixation and sequentially developed with Cy3-labeled goat anti-rabbit IgG (H + L; Jackson ImmunoResearch Laboratories).

Mouse Tumor Models

Seven-week-old BALB/c female nude mice were obtained from CLEA Japan. A total of 1.0×10^5 cells of human glioblastoma line U87ΔEGFR were suspended on ice in 5 μL RPMI (-FCS) and sequentially transplanted into brain by direct injection using a stereotaxis device (Narishige Scientific Instrument Lab). Survival was assessed in 10 peptide-treated mice as measured against

[7] Supplementary material for this article is available at Molecular Cancer Therapeutics Online (http://mct.aacrjournals.org/).

PBS-treated mice. Tetramethylrhodamine-conjugated low molecular weight dextran (~10 kDa; 20 mg/mL; Invitrogen/Molecular Probes) was i.v. injected into brain tumor-stricken mice to observe brain histologic profiles (21). Animal studies in the present work were approved by the Okayama University Graduate School of Medicine, Dentistry and Pharmaceutical Sciences Subcommittee on Animal Research. All mouse procedures, euthanasia and surgery, including glioma transplantations and peptide injections, were done painlessly or under anesthesia, within strict guidelines of the Experimental Animal Facility of Okayama University Graduate School of Medicine, Dentistry and Pharmaceutical Sciences.

Histologic Examination

Brain tissues were fixed overnight in 10% buffered formalin, embedded in paraffin, and sectioned in 5 μm slices. Sections were stained with H&E or with a rabbit polyclonal antibody reactive to Ki-67 (Novocastra Laboratories) following immunohistochemistrical method. For signal development with the Ki-67 antigen, Envision+ was used according to manufacturer protocol (DAKOCytomation).

Statistic Analysis

Statistical significance was calculated using the statistics software package Statview (SAS Institute). Survival curves were generated by the Kaplan-Meier method. $P < 0.05$ was considered statistically significant.

Results

Functional Properties of the Wr-T Peptide/Protein Transporter

First, we characterized the detailed functions of the 30–amino acid peptide/protein transporter ''Wr-T.'' As we reported previously, Wr-T was generated from prototypal peptide ''pep-1,'' which showed highly proficient intracellular peptide/protein delivery by forming a cell-permeable complex with the cargo peptide/protein (11, 12). Tryptophan-rich motif WWE/T of pep-1 was reported to dock with a cargo protein and form a transporter/cargo complex, which was expanded to a three-repeat sequence in Wr-T. Three amino acids, Gly-Pro-Gly, were additionally inserted as a spacer between the protein-docking domain and a PTD comprising nine poly-D-arginines (Fig. 1). When the repeated tryptophan-rich motif was truncated as peptide A in Fig. 1, intracellular delivery of the β-Gal tetramer (total molecular weight: ~485 kDa) to HeLa-S3 cells was markedly disrupted. Similarly, peptide B, which lacked a Gly-Pro-Gly spacer, abrogated the intracellular incorporation of β-Gal with the dose indicated in Fig. 1. Peptide C, which replaced the nine D-arginine PTD of Wr-T with the SV40 nuclear localization signal, PKKKRKV, abolished efficient delivery of β-Gal (Fig. 1). Thus, the entire amino acid sequence encoded by Wr-T was required to fully function as a protein transporter with respect to efficient docking of cargo protein and cell permeability.

INK4 Family Tumor Suppressor Background in Aggressive Glioblastoma Cells and Dual Uptake of p14 and p16 Functional Peptides

Before establishing an *in vitro* peptide targeting model for human glioblastoma cells, endogenous expression of INK4 family genes in two glioblastoma cell lines, U87ΔEGFR and Gli36ΔEGFR, was examined by reverse transcription-PCR (Fig. 2A). These glioblastoma lines were highly proliferative *in vitro*, due to introduction of a gain-of-function *EGFR* mutation, consistent with clinical aggressiveness (17, 18). Consequently, they revealed expressional losses in $p14^{ARF}$ and $p16^{INK4a}$ in addition to p15 and/or p18 (Fig. 2A, *left*). Cdk4, the target for $p16^{INK4a}$, was strongly expressed in both U87ΔEGFR and Gli36-ΔEGFR, and expression of Hdm2, a target for $p14^{ARF}$, was also pronounced (Fig. 2A, *right*). Accordingly, we attempted to restore p14 and p16 gene function simultaneously by introducing both p14 and p16 functional peptides (3 μmol/L final concentration for each) mixed with Wr-T (3.5 μmol/L for each cargo peptide; see Materials and Methods; Fig. 2C, *left*). The cargo, newly designed to restore tumor suppressor gene $p14^{ARF}$ function, we term p14-1C: it is a novel 37–amino acid structure containing a NH_2-terminal helical sequence, RRFLVTLRIRRA, fused to helix VRVFVVHIPR from human $p14^{ARF}$ via the Gly-Pro-Gly spacer, which in turn is bonded to nine poly-D-arginines (Fig. 2B). The two NH_2-terminal helical domains of p14 are known to form a core essential to p14/Hdm2 binding, responsible for preventing p53 degradation by Hdm2-mediated ubiquitination (15, 22). Thus, the p14-1C peptide was expected to stabilize p53 by competing away Hdm2, with which p53 would otherwise interact. Ectopic expression of $p14^{ARF}$ has been reported to activate p53 and p21 (22). The ''p16-MIS'' peptide for p16 restoral was also synthesized to be used for Wr-T-mediated peptide delivery because its function was already shown in the previous study (Fig. 2B; ref. 11). Then, we carried out initial optimization for multiple peptide transport on U87ΔEGFR cells by treating with both Wr-T/p14-1C and Wr-T/p16-MIS complexes (Fig. 2C, *left*), and live cells were examined under inverted fluorescence microscope for whether coexistence of Cy3 and FITC signals in the same cell was clearly observed. Resultant images 24 h after treatment showed intense Cy3 and FITC signals, which were p14-1C and p16-MIS derived and are observed simultaneously in the same viable U87ΔEGFR cell as well as the apoptotic cell, showing efficient intracellular transport of dual peptides by Wr-T (Fig. 2C, *right*). Because p16-MIS peptide intracellularly delivered by Wr-T was shown previously to block the cell cycle (11), we examined whether newly designed p14-1C peptide also functioned in a target-specific manner within the uptaken cells. Immunoblots (Fig. 2D) probed with anti-p53 monoclonal antibody showed substantial recovery of p53 levels in Wr-T (7 μmol/L)/p14-1C-treated U87ΔEGFR cells in a time- and dose-dependent manner (Fig. 2D). This effect was further supported by increases in p21, a known p53-induced target (Fig. 2D).

Therapeutic Peptide Action against Human Glioblastoma Cells Lacking p14 and p16 Expression

Based on these results, we tested for glioblastoma growth suppression by Wr-T-mediated p14 and p16 dual-peptide delivery in U87ΔEGFR cells in comparison with introducing p14 or p16 by single-peptide delivery. At 120 h post-introduction, normalized absorbance values from MTT assays showed that dual-complex treatment with Wr-T/p16-MIS (3.5 + 3 μmol/L) and Wr-T/p14-1C (3.5 + 3 μmol/L) dramatically suppresses U87ΔEGFR growth by 95% within 72 h compared with single complexes of Wr-T/p16-MIS (7 + 6 μmol/L) or Wr-T/p14-1C (7 + 6 μmol/L) alone, which inhibited growth by only 30% and 37%, respectively (Fig. 3A, *left*). Moreover, this strong inhibitory effect by the dual-peptide complexes was strongly persistent for 120 h, whereas inhibition by the single-peptide complex gradually diminished in a time-dependent manner. Similarly, more enhanced growth suppression was observed when treatments with these dual-peptide complexes were repeated 48 h after initial peptide treatment, yielding >97% suppression (data not shown). The result (Fig. 3A) suggested that nearly complete blockade against proliferation of aggressive U87ΔEGFR was possible only when these tumor suppressor functions jointly recovered, at peptide dosages that would have produced only 30% to 40% suppression in the single-peptide protocols. Flow cytometric analysis using Annexin V showed that ~72% of the dual-peptide complex-treated cells had already triggered apoptosis by 24 h, whereas groups treated with Wr-T alone, Wr-T/p14-1C, or Wr-T/p16 yielded no significant

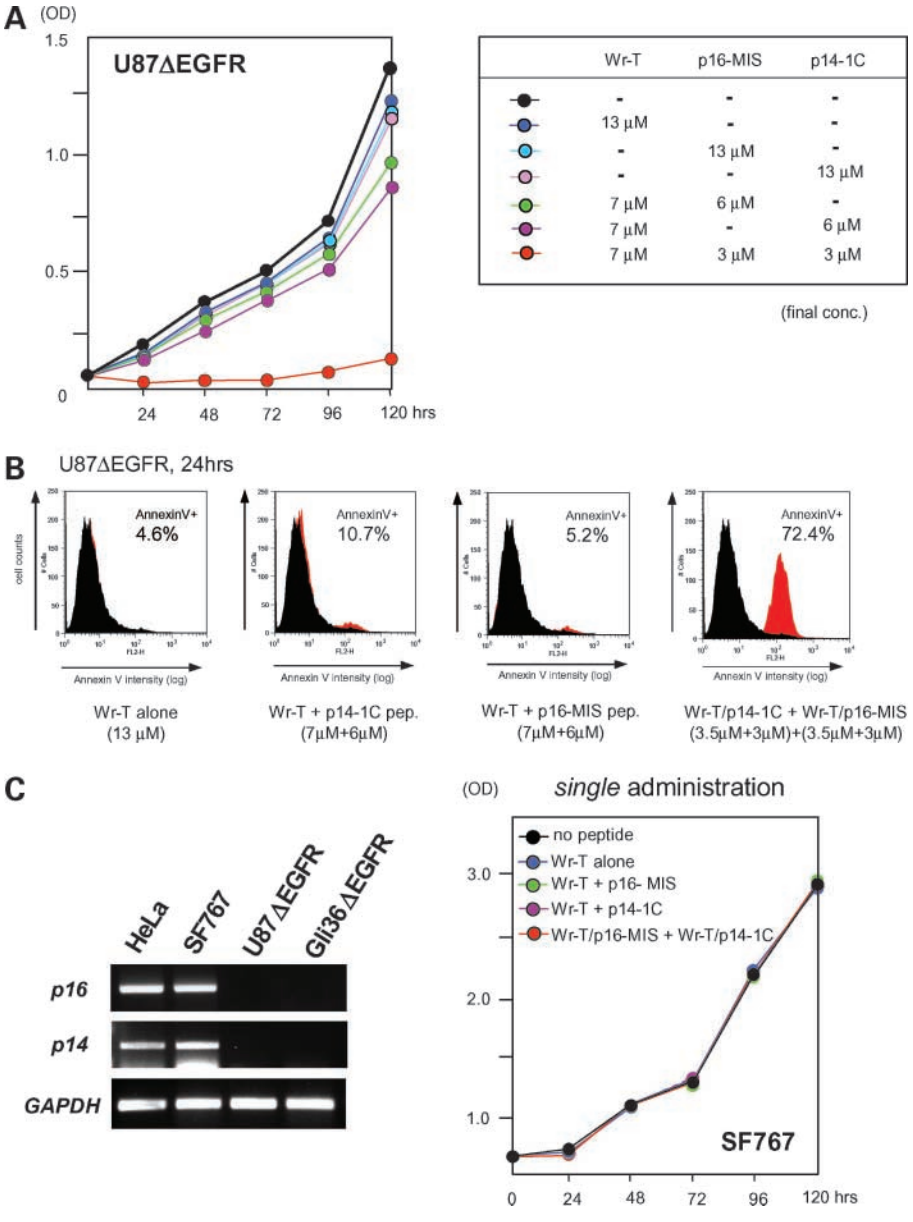

Figure 3. Growth inhibition of U87ΔEGFR by dual-peptide delivery. **A,** MTT assay on untreated U87ΔEGFR cells (initially 2×10^4), Wr-T alone, p16-MIS alone, p14-1C alone, Wr-T/p16-MIS, Wr-T/p14-1C, and Wr-T/p16-MIS + Wr-T/p14-1C complex with indicated concentrations shown in the table. Time points were taken in triplicate; graphed values are average absorbance. **B,** fluorescence-activated cell sorting analysis using Cy3-labeled Annexin V 24 h after peptide treatment. *Red,* population of Annexin V–positive cells. **C,** SF767 glioma cell line was resistant to the p14 and p16 peptide complex. *Left,* SF767 cells retain endogenous expression of *p16* and *p14* as detected by reverse transcription-PCR; *right,* MTT assay on peptide-treated SF767 cells. Wr-T alone (13 μmol/L), Wr-T (7 μmol/L)/p16-MIS (6 μmol/L), Wr-T (7 μmol/L)/p14-1C (6 μmol/L), Wr-T (3.5 μmol/L)/p16-MIS(3 μmol/L) + Wr-T (3.5 μmol/L)/p14-1C (3 μmol/L).

apoptosis (Fig. 3B). This dual-peptide delivery showed significant inhibitory action against other human native glioblastoma cell lines such as U87MG, AO2, SK-MG-1, and T98, which were negative for both p14 and p16 expression, and appeared to be also partially effective on weakly p14- and p16-positive glioblastoma, U251 (Supplementary Fig. S1A and B).[7] Exceptionally, little or no suppression was observed in another human glioma cell line, SF767, which strongly expressed endogenous p14 and p16, when treated by the dual peptides with the same dosage as U87ΔEGFR (Fig. 3C), suggesting that the regime is p14 and p16 specific. These results indicate that our p14 and p16 targeting system may be not as successful against tumors strongly expressing endogenous p14/p16 probably because their growth is independent of p14/p16 pathways. Unexpectedly, when dual-peptide targeting was applied to another glioblastoma cell line, p14- and p16-negative Gli36ΔEGFR (Fig. 2A), it suppressed proliferation by only 52%, which was apparently less effective than the 95% inhibition of U87ΔEGFR cells (Fig. 4A). Further consideration of earlier mutational findings (17) appears to shed light on the behavior of Gli36ΔEGFR, which we confirmed bears a missense mutation in exon 7 of *p53*, a R248L substitution (Fig. 4B, *left*). DNA sequencing showed no genetic mutation within *p53* ORF of U87ΔEGFR and SF767 cell lines (data not shown). UV-irradiated Gli36ΔEGFR underwent apoptosis due to UV-induced DNA damage. When we subjected WT-*p53*-transfected Gli36ΔEGFR cells to a range of UV doses (no UV, 10, and 15 J/m^2 UV 12 h post-transfection), >60% of cells exposed to 10 J/m^2 UV were positive for anti-active caspase-3 antibody and began showing apoptosis-associated morphologic shrinkage within 12 h (Fig. 4C). Furthermore, >70% of WT-p53-expressing cells entered apoptosis 12 h following 15 J/m^2 UV exposure (Fig. 4C, *left* and *middle*). Notably, unlike the WT-p53-transfected cells, mutant R248L *p53*-transfected cells were significantly resistant to UV-induced apoptosis (27% of caspase-3-positive cells at 10 J/m^2 UV and 33% at 15 J/m^2 UV exposure), which suggested that the R248L mutation impaired proapoptotic *p53* function (Fig. 4C, *middle*). Taken together, our results indicate that this *p53* mutation is expected to impair induction of downstream apoptotic molecules such as p21, Fas ligand, Bax, 14-3-3, or GADD45 (Fig. 4C, *right*). In view of the Gli36ΔEGFR *p53* alteration, we sought to restore p21^{CIP1} function instead of p14 by targeting them with functional peptide p21-S154A (14) using a Wr-T/p16-MIS protocol for growth suppression. Fluorescence microscopy showed simultaneous Wr-T (7 μmol/L)–mediated transport of FITC-labeled p16-MIS (3 μmol/L) and Atto651-labeled p21-S154A (3 μmol/L) peptides (Fig. 4D, *top left*). Fluorescence-activated cell sorting analysis using propidium iodide revealed that incorporation of p21-S154A (6 μmol/L) peptide combined with Wr-T (7 μmol/L) induced ostensible p21-specific inhibition of the cell cycle as reflected by a substantial increase in the sub-G_1 phase (Fig. 4D, *middle left, red arrow*; ref. 23). Fluorescence-activated cell sorting analysis showed significant increases in Annexin V–positive dual-peptide-treated cells 48 h post-treatment as an indication of sub-G_1-phase cells eventually undergoing apoptosis (Fig. 4D, *bottom*). Efficacy was shown by MTT assay, where p16/p21 dual targeting was much more effective than p16 or p21 single targeting at each dosage indicated, which shows a surprising reduction of Gli36ΔEGFR proliferation to within 3% of untreated controls (Fig. 4C, *right*). The Wr-T-delivered p21-S154A peptide even showed antiproliferative effects on SF767 glioma cells, which were resistant to p14 and p16 peptide treatment, in a dose-dependent manner (Supplementary Fig. S1C).

Brain Tumor Suppression by *In vivo* Dual-Peptide Targeting

Our results thus far encouraged us to apply our system to the experimental therapeutic challenge of human glioblastomas *in vivo*. We generated a mouse brain tumor model by transplanting 1 × 10^5 cells of human glioblastoma U87ΔEGFR into the cerebrum of 7-week-old BALB/c nude mice (Fig. 5A, *scheme*) using a stereotaxis device. When tumors grew to a maximum of ~3 mm in diameter (~100 mm^3 in volume) at 5 days, mixtures of Wr-T/p16 and Wr-T/p14-1C complexes (20 nmol Wr-T mixed with 20 nmol of each cargo peptide) were injected i.v. through the heart. Tumors were Ki-67 positive, suggesting rapid proliferation, and without treatment generally grew to occupy the entire hemispheres of the brain at ~20 days post-implantation, thus killing the animals (Fig. 5B). We visualized blood-brain barrier integrity by i.v. injecting 20 mg/mL tetramethylrhodamine-labeled low molecular weight dextran (molecular weight ~10 kDa), which readily accumulated in the malignancy, showing blood-brain barrier impairment at the tumor site (Fig. 5C). Based on these observations, we injected the peptide complexes through the right ventricle of the heart for blood-borne transit to the brain. Significantly, the circulating peptides concentrated at the tumor site in much the same distribution pattern as the dextran after 24 h of injection (Fig. 5D). Although very small amounts of peptide were seen in surrounding nonneoplastic tissue, the tissue remained histologically normal, which suggested that these peptides disseminated non-invasively (Fig. 5E). Although autopsies revealed that all dual-peptide-treated mice eventually died from hemispheric occupying tumor as in Fig. 5B (data not shown), the treatment regimen was highly significant to prolonging overall survival. Accordingly, we statistically evaluated the therapeutic benefit to the mice using Kaplan-Meier nonparametric analysis and hence the *in vivo* potency of the Wr-T-based dual targeting against the invading human tumor. Our findings indicate that dual-peptide-treated mice as a group experienced longer average survival, by a statistically robust factor of 1.5, over the nontreated group, due to growth retardation of the tumor by the dual antitumor peptides (Fig. 5F).

Discussion

Recent molecular targeting techniques using PTD fusion peptide have gained considerable attention for their

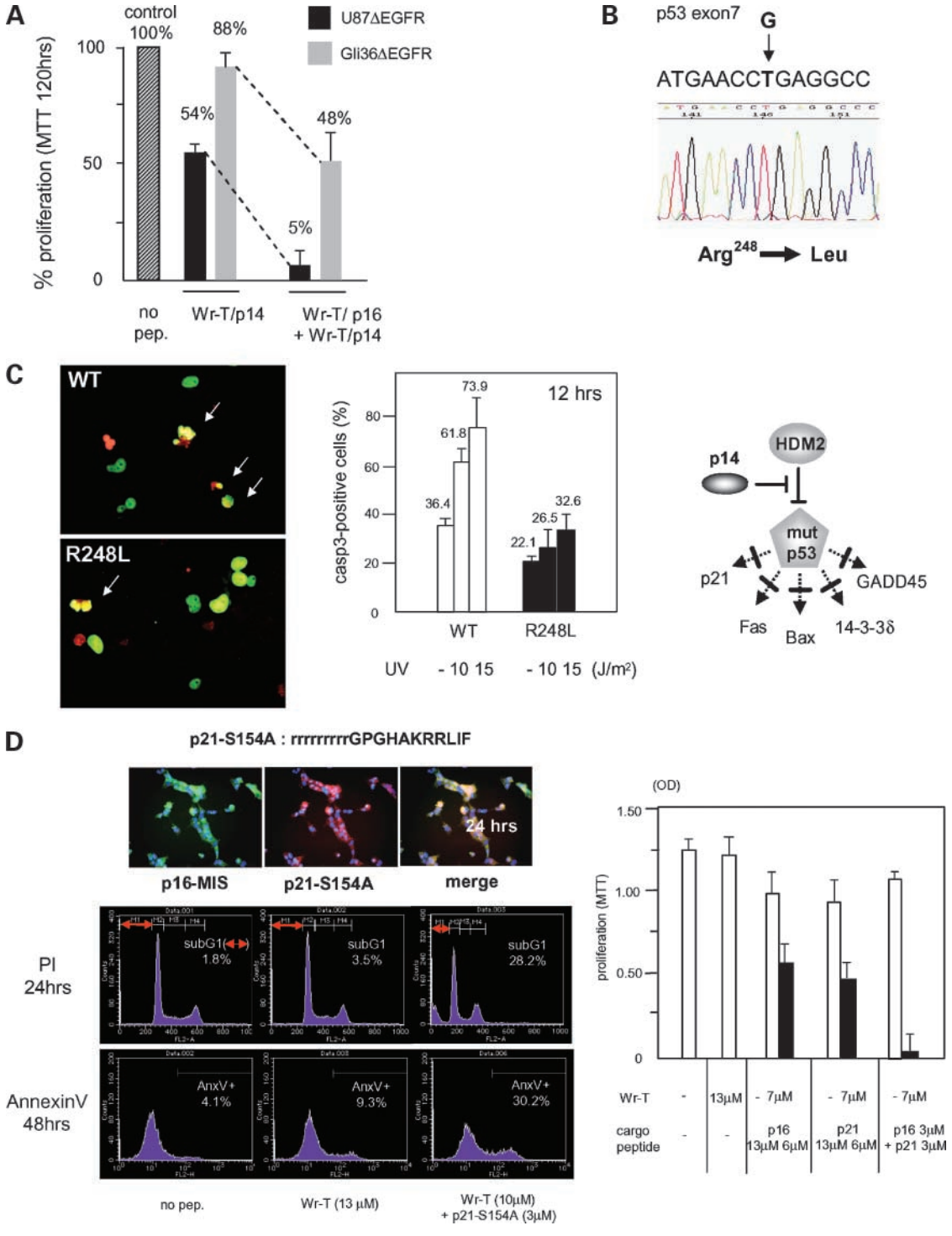

Figure 4. Gli36ΔEGFR bearing a *p53* mutation, thereby resistant to p14-1C peptide but sensitive to the combination of p21-S154A and p16-MIS peptide. **A,** percent proliferation of peptide-treated cells (initially 2×10^4) from MTT assay 120 h after treatment. Wr-T/a cargo complex: Wr-T (3.5 μmol/L)/p14-1C (3 μmol/L), Wr-T (3.5 μmol/L)/p16-MIS (3 μmol/L). **B,** point mutation (R248L) at exon 7 of *p53* in Gli36ΔEGFR from genomic sequence (*left*). **C,** response to UV exposure of Gli36ΔEGFR bearing WT-p53 or R248L of *p53* mutation. *Left,* anti-active caspase-3 staining after UV exposure; *middle,* percentage of UV-induced apoptosis in each transfected line post-UV treatment; *right, p53* R248L mutation ostensibly disables downstream induction of proapoptotic genes including $p21^{CIP1}$. **D,** amino acid sequence of the p21 functional peptide, p21-S154A, and joint uptake of Wr-T/p16-MIS and Wr-T/p21-S154A complexes by Gli36ΔEGFR cells. p16-MIS (FITC), p21-S154A (Atto655). *Top left,* function of p21-S154A peptide in cell cycle blockade (increase of sub-G_1 phase) for a 24-h incubation and induction of apoptosis 48 h post-treatment shown by FACScan analysis (*middle left,* propidium iodide staining; *bottom left,* Cy3-Annexin V); *Right,* growth inhibition of Gli36ΔEGFR (initially 2×10^4) after 120 h of treatment by the indicated concentration of each peptide.

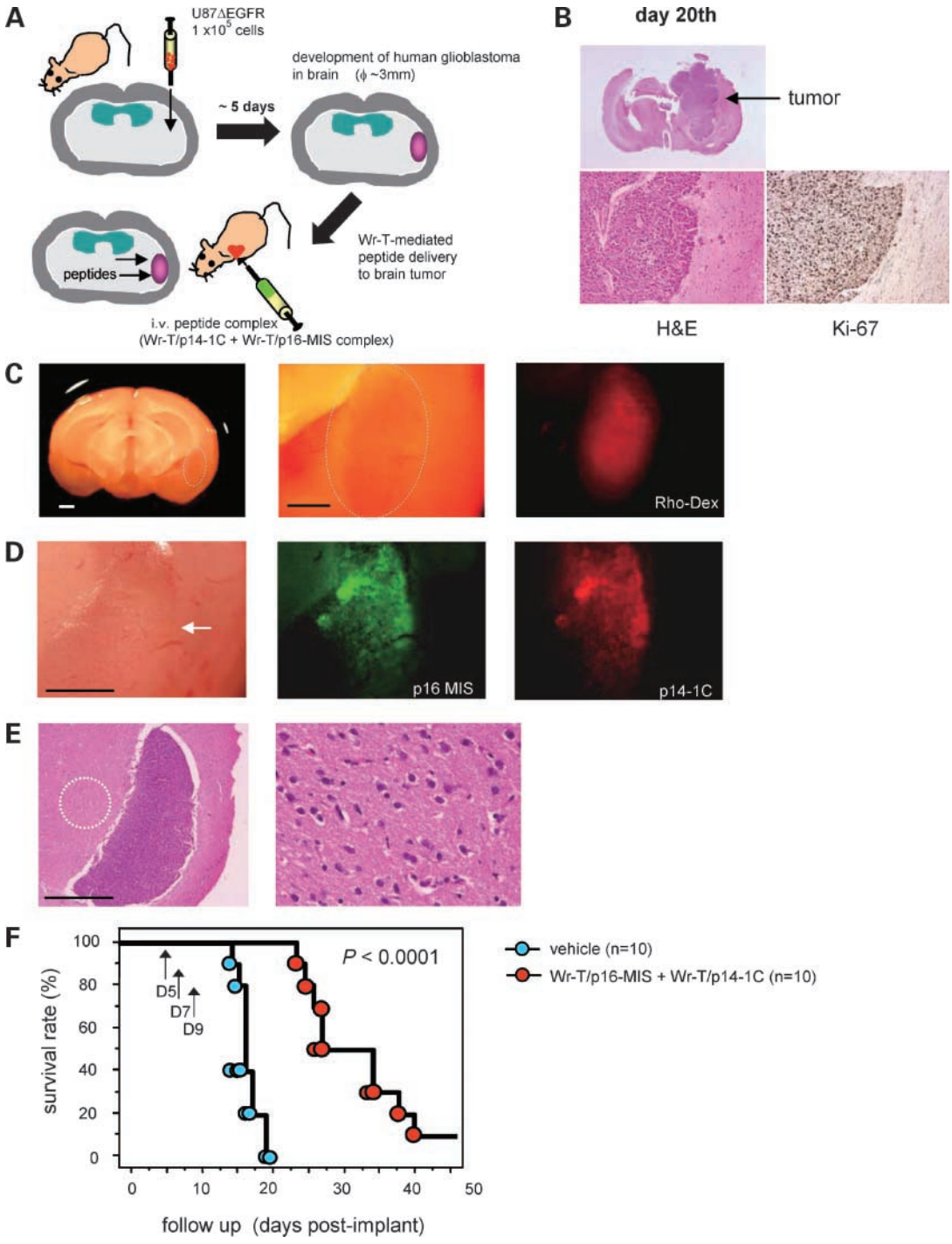

Figure 5. Utility of dual Wr-T/p16-MIS and Wr-T/p14-1C peptide delivery for transplanted human glioblastoma *in vivo*. **A,** schematic of *in vivo* delivery of dual-peptide complexes in a mouse model. The peptide complexes were injected into the heart when the tumor had grown to 3 mm in diameter. **B,** development of human glioblastoma in mouse brain 20 d after injection of cells. Ki67 immunostaining indicated that >60% of cells were positive. **C,** blood-brain barrier breakdown at the tumor site as shown by accumulation of low molecular weight dextran (*Rho-Dex*). Low molecular weight dextran was injected into the heart when the brain tumor had grown to 3 mm in diameter. *Dotted circles,* transplanted tumor. Bar, 1 mm. **D,** accumulation of both p16 and p14 peptides in the tumor 24 h after peptide injection. Mixtures of Wr-T/p16-MIS and Wr-T/p14-1C complexes were injected at 5 d post-transplantation (20 nmol FITC-p16-MIS or 20 nmol Cy3-p14-1C mixed with 20 nmol Wr-T, respectively). *Arrow,* tumor. Bar, 1 mm. **E,** histologic examination of the same brain tissue shown in Fig. 4D, focusing on the normal tissue at the tumor boundary (*left*). Hyperview of the area within the *dotted circle* (*right*). Bar, 1 mm. **F,** Kaplan-Meier curves for overall survival of animals treated three times with a mixture of the peptide complex (at days 5, 7, and 9 after transplantation). Dual-peptide complexes were injected at each indicated time point. [vehicle (PBS) group: $n = 10$; Wr-T/p16-MIS + Wr-T/p14-1C group: $n = 10$]. Prolonged survival of the dual-peptide-treated mice was statistically significant ($P < 0.0001$).

therapeutic potential. In this regard, various PTD agents such as HIV-1 TAT, pAnt(penetratin), SV40NLS, have been investigated for delivering proteins into human cells (24, 25). However, aside from basic cell permeability, success of PTD fusion therapies depends on the efficiency of incorporation into target cells. We considered intracellular delivery based on forming a transporter/cargo peptide complex to be highly relevant to this problem because our system raises efficiencies of cargo peptide uptake >10-fold relative to uncomplexed PTD-fused single peptide as we showed previously (11). Although other new molecular targeting agents such as small-molecule inhibitors (e.g., gefitinib to HER-1, imatinib to BCR-ABL, and bortezomib to proteasome) and the humanized antibodies (e.g., rituximab to CD20 and bevacizumab to vascular endothelial growth factor) have widened the scope of therapies (1–4, 26–28), these single-molecule targeting therapies have often generated tumor escape mutants, presenting serious relapse issues (29–31). Here, we showed greatly enhanced suppression of aggressive glioblastoma cells by delivery of dual tumor suppressor peptides with a peptide/protein transporter ''Wr-T.'' This complex-forming system offers a wide choice in a cargo peptide/protein, prolonged activity, and markedly improved efficiencies over the previous peptide delivery systems (11). Our system is founded on two functional peptides having distinct amino acid sequences, p16-MIS and p14-1C or p21-S154A, and its implementation yielded drastic inhibition of glioblastoma growth. Specifically, 95% suppression against U87ΔEGFR was achieved within 72 h with only single treatments of p14/p16 dual functional peptides, and 97% suppression was observed against Gli36ΔEGFR after 120 h by intracellular p16/p21 dual-peptide delivery *in vitro*. This antitumor effect was rapidly initiated because dramatic apoptosis increases were observed within 24 h in the peptide-treated U87ΔEGFR cells by FACScan analysis using Annexin V. We believe this speed of action of p14 and p16 dual delivery, giving rise to extensive (72%) apoptosis where no significant apoptosis was seen with single targeting, is due to synergistic growth inhibition derived from both p16-mediated cell cycle arrest and p14-mediated activation of p53 function (32, 33). This accounts for the consistent synergism, rather than additivity, from our dual-peptide suppression versus single-peptide regimes. Similarly, efficient suppression (from 94% to 61%) was observed in other nongenetically engineered native glioblastoma cell lines, which lack both *p14* and *p16* expression as shown in Supplementary Fig. S1A and B. Among the glioblastoma cell lines examined, this inhibition varied somewhat because of probable differences in genetic background affecting antiapoptotic molecules and/or INK4 family members. This strongly targeted suppressive effect carries further benefits for dosage minimization, which will be clinically important to controlling unfocussed cytotoxicity and injurious side effects. In this regard, typical tumor-suppressive doses of previous studies ranged from 200 to >2,000 nmol in cancerous mice (34–37); however, here we successfully employed only 20 nmol of the p16 or p14 peptide combined with 40 nmol Wr-T. Moreover, prolonged survival in tumor-bearing mice was achieved with only a three-time i.v. injection protocol at 48-h intervals, whereas the most comparable work elsewhere entailed peptide injections in numerous stages (>10 times; refs. 34–37), at closer intervals (34), or in a more localized and invasive manner (36, 37). Another significant advantage we showed is that *in vivo* the Wr-T transporter-mediated system offers long-range delivery far from the site of introduction, suggesting locational versatility; this is especially advantageous for malignant tumors including glioblastomas in view of the functional impairment of tumor-generated blood vessels as shown in the blood-brain barrier at tumor site. Furthermore, one of the most important issues in the drug delivery systems is the side effect such as nonspecific toxicities from extrinsic agents *in vitro* and *in vivo*. The Wr-T/a cargo peptide delivery system is fundamentally applicable to broad ranges of human cell types due to the inherent non-type-specific permeability imparted by the poly-arginine PTD to Wr-T. As an *in vitro* assay, the p14 and p16 dual-peptide complexes were incorporated into both nonneoplastic cells (e.g., PBMC, mouse hepatocytes, and normal human fibroblasts) and neoplastic cells (e.g. HeLa and Hs578; Supplementary Fig. S2*A*). However, with the same dual-peptide complex dosage, only minimum cytotoxicity was observed in PBMC and hepatocytes *in vitro* because of their endogenous p14 and p16 expressions. Significantly, fluorescence-activated cell sorting analysis with Annexin V showed that 92.2% of PBMC were viable 24 h post-introduction, with no significant increase of cleaved poly(ADP-ribose) polymerase detected in hepatocytes by immunoblotting (Supplementary Fig. S2B-E).[7] In contrast to nonneoplastic cells, tumor cell lines such as HeLa and especially the *p14/p16* double-negative breast cancer cell, Hs578, underwent apoptosis as shown by comparable increases in cleaved poly(ADP-ribose) polymerase, indicating that our system may be available to other *p14/p16*-negative malignancies (Supplementary Fig. S2D and E). *In vivo* examination of the peptide-treated mice 72 h post-injection also revealed that the dual-peptide complexes penetrated various tissues including liver, kidney, and spleen. Histologic examination of these organs showed normal architectures with no significant cellular damage, where fluorescent signals derived from both peptides were detected (Supplementary Fig. S3).[7] In conclusion, our study shows the potential of the Wr-T-mediated dual-peptide delivery system for extensive growth suppression of human glioblastoma cells, allowing minimally invasive, combined recovery of dual tumor suppressor function. This antitumor strategy should be clinically relevant to a variety of currently intractable malignancies besides glioblastomas. Additional detailed investigations will be required to ensure intracellular stability, higher efficiency, and reduced toxicity and to develop a systematic targeted therapy against the unresponsive malignancies.

Disclosure of Potential Conflicts of Interest

No potential conflicts of interest were disclosed.

Acknowledgments

We thank K.V. Myrick (Department of Molecular and Cellular Biology, Harvard University) for critical reading of the article and Dr. A. Natsume (Department of Neurosurgery, Nagoya University) for kindly providing human glioma cell lines.

References

1. Fire A, Xu SQ, Montgomery MK, Kostas SA, Driver SE, Mello CC. Potent and specific genetic interference by double-stranded RNA in *Caenorhabditis elegans*. Nature 1998;392:806 – 11.

2. Reff ME, Carner K, Chambers KS, et al. Depletion of B cells *in vivo* by a chimeric mouse human monoclonal antibody to CD20. Blood 1994;83: 435 – 45.

3. Herbst RS, Fukuoka M, Baselga J. Gefitinib—a novel targeted approach to treating cancer. Nature 2004;4:956 – 65.

4. Pao W, Miller VA. Epidermal growth factor receptor mutations, small-molecule kinase inhibitors, and non-small-cell lung cancer. J Clin Oncol 2005;23:2556 – 68.

5. Mellinghoff IK, Wang M, Vivanco I, et al. Molecular determinants of the response of glioblastomas to EGFR kinase inhibitors. N Eng J Med 2005; 353:2012 – 24.

6. Newcomb EW, Alonso M, Sung T, et al. Incidence of p14ARF gene deletion in high-grade adult and pediatric astrocytomas. Hum Pathol 2000; 31:115 – 9.

7. Simon M, Koster G, Menon AG, Schramm J. Functional evidence for a role of combined CDKN2A (p16-14(ARF))/CDKN2B (p15) gene inactivation in malignant gliomas. Acta Neuropathol (Berl) 1999;98:444 – 52.

8. Saxena A, Shriml LM, Dean M, Ali IU. Comparative molecular genetic profiles of anaplastic astrocytomas/glioblastomas multiforme and their subsequent recurrences. Oncogene 1999;18:1385 – 90.

9. Adachi Y, Chandrasekar N, Kin Y, et al. Suppression of glioma invasion and growth by adenovirus-mediated delivery of a bicistronic construct containing antisense uPAR and sense p16 gene sequences. Oncogene 2002;21:87 – 95.

10. Labuhn M, Jones G, Speel EJ, et al. Quantitative real-time PCR does not show selective targeting of p14(ARF) but concomitant inactivation of both p16(INK4A) and p14(ARF) in 105 human primary gliomas. Oncogene 2001;20:1103 – 9.

11. Kondo E, Seto M, Yoshikawa K, Yoshino T. Highly efficient delivery of p16 anti-tumor peptide into aggressive leukemia/lymphoma cells using a novel transporter system. Mol Cancer Ther 2004;3:1623 – 30.

12. Morris MC, Depollier J, Mery J, Heitz F, Divita G. A peptide carrier for the delivery of biologically active proteins into mammalian cells. Nat Biotechnol 2001;19:1173 – 6.

13. Fahraeus R, Lain S, Ball KL, Lane DP. Characterization of the cyclin-dependent kinase inhibitory domain of the INK4 family as a model for a synthetic tumour suppressor molecule. Oncogene 1998;16:587 – 96.

14. Zheleva DI, McInnes C, Gavine AL, Zhelev NZ, Fischer PM, Lane DP. Highly potent p21(WAF1)-derived peptide inhibitors of CDK-mediated pRb phosphorylation: delineation and structural insight into their interactions with cyclin A. J Pept Res 2002;60:257 – 70.

15. Kontopidis G, Andrews MJ, McInnes C, Cowan A, Powers H, Innes L. Insights into cyclin groove recognition: complex crystal structures and inhibitor design through ligand exchange. Structure 2003;11:1537 – 46.

16. DiGiammarino EL, Filippov I, Weber JD, Bothner B, Kriwacki RW. Solution structure of the p53 regulatory domain of the p19Arf tumor suppressor protein. Biochemistry 2001;40:2379 – 86.

17. Abe T, Terada K, Wakimoto H, et al. PTEN decreases *in vivo* vascularization of experimental gliomas in spite of proangiogenic stimuli. Cancer Res 2003;63:2300 – 5.

18. Abe T, Wakimoto H, Bookstein R, et al. Intra-arterial delivery of p53-containing adenoviral vector into experimental brain tumors. Cancer Gene Ther 2002;9:228 – 35.

19. Delmas C, Heliez C, Cohen-Jonathan E, et al. Farnesyltransferase inhibitor, R115777, reverses the resistance of human glioma cell lines to ionizing radiation. Int J Cancer 2002;100:43 – 8.

20. Fink JR, LeBien TW. Novel expression of cyclin-dependent kinase inhibitors in human B-cell precursors. Exp Hematol 2001;29:490 – 8.

21. Nitta T, Hata M, Gotoh S, et al. Size-selective loosening of the blood-brain barrier in claudin-5-deficient mice. J Cell Biol 2003;161:653 – 60.

22. Stott FJ, Bates S, James MC, et al. The alternative product from the human CDKN2A locus, p14(ARF), participates in a regulatory feedback loop with p53 and MDM2. EMBO J 1998;17:5001 – 14.

23. Meinhardt G, Roth J, Hass R. Activation of protein kinase C relays distinct signaling pathways in the same cell type: differentiation and caspase-mediated apoptosis. Cell Death Differ 2000;7:795 – 803.

24. Schwarze SR, Ho A, Vocero-Akbani A, Dowdy SF. *In vivo* protein transduction: delivery of a biologically active protein into the mouse. Science 1999;285:1569 – 72.

25. Perez F, Joliot A, Bloch-Gallego E, Zahraoui A, Triller A, Prochiantz A. Antennapedia homeobox as a signal for the cellular internalization and nuclear addressing of a small exogenous peptide. J Cell Sci 1992;102: 717 – 22.

26. Hughes TP, Kaeda J, Branford S, et al. International Randomised Study of Interferon versus STI571 (IRIS) Study Group. Frequency of major molecular responses to imatinib or interferon α plus cytarabine in newly diagnosed chronic myeloid leukemia. N Engl J Med 2003;349:1423 – 32.

27. Adams J. Proteasome inhibition in cancer: development of PS341. Semin Oncol 2001;28:613 – 9.

28. Presta LG, Chen H, O'Connor SJ, et al. Humanization of an anti-vascular endothelial growth factor monoclonal antibody for the therapy of solid tumors and other disorders. Cancer Res 1997;57:4593 – 9.

29. Janne PA, Engelman JA, Johnson BE. Epidermal growth factor receptor mutations in non-small-cell lung cancer: implications for treatment and tumor biology. J Clin Oncol 2005;23:3227 – 34.

30. Pao W, Miller VA, Politi KA, et al. Acquired resistance of lung adenocarcinomas to gefitinib or erlotinib is associated with a second mutation in the EGFR kinase domain. PLoS Med 2005;2:e73.

31. Balak MN, Gong Y, Riely GJ, et al. Novel D761Y and common secondary T790M mutations in epidermal growth factor receptor-mutant lung adenocarcinomas with acquired resistance to kinase inhibitors. Clin Cancer Res 2006;12:6494 – 501.

32. Sandig V, Brand K, Herwig S, Lukas J, Bartek J, Strauss M. Adenovirally transferred p16INK4/CDKN2 and p53 genes cooperate to induce apoptotic tumor cell death. Nat Med 1997;3:313 – 9.

33. Kim SK, Wang KC, Cho BK, et al. Interaction between p53 and p16 expressed by adenoviral vectors in human malignant glioma cell lines. J Neurosurg 2002;97:143 – 50.

34. Cao G, Pei W, Ge H, et al. *In vivo* delivery of a Bcl-xL fusion protein containing the TAT protein transduction domain protects against ischemic brain injury and neuronal apoptosis. J Neurosci 2002;22:5423 – 31.

35. Snyder EL, Meade BR, Saenz CC, Dowdy SF. Treatment of terminal peritoneal carcinomatosis by a transducible p53-activating peptide. PLoS Biol 2004;2:E36. Epub 2004 Feb 17.

36. Hiromura M, Okada F, Obata T, et al. Inhibition of Akt kinase activity by a peptide spanning the βA strand of the proto-oncogene TCL1. J Biol Chem 2004;279:53407 – 18.

37. Mai JC, Mi Z, Kim SH, Ng B, Robbins PD. A proapoptotic peptide for the treatment of solid tumors. Cancer Res 2001;61:7709 – 12.